Simulated neutron-induced fission cross sections for various Pu, U, and Th isotopes

W. Younes* and H. C. Britt
Lawrence Livermore National Laboratory, Livermore, California 94551, USA
(Received 1 April 2003; published 18 September 2003)

Neutron-induced fission cross sections have been extracted for targets of ^{240,241,243}Pu, ^{234,236,237,239}U, and ^{231,233}Th from $E_n = 100$ keV to ≈ 2.5 MeV using surrogate (t,pf) fission-probability data and a detailed statistical model to compensate for the difference between neutron-induced and (t,p) reactions. This paper extends the results of previous work on the ^{235}U(n,f) cross section, which serves as a proof-of-principle study. The (n,f) cross sections are compared to earlier estimates based on the same surrogate data, but obtained using a more simplistic approach. The cross sections are also compared to accepted values where direct measurements exist and are consistently accurate to within 20% below $E_n \approx 0.5$ MeV and 10% at higher energies. The case of the ^{237}U(n,f) cross section, simulated from surrogate (t,pf) data, is investigated in greater detail to reconcile contradictory measurements in the literature.

DOI: 10.1103/PhysRevC.68.034610 PACS number(s): 25.85.Ec, 25.40.−h, 25.85.Ge

I. INTRODUCTION

Surrogate reactions, coupled with modeling, can be used to estimate nuclear properties in systems that may be important in some environments, but for which appropriate targets may not be available for a direct measurement. One example of this technique is the direct-reaction fission-correlation measurement using the reaction (t,pf) on a target of mass A to simulate neutron-induced fission on a target of mass $A+1$.

In a previous paper [1], a model was developed to convert fission-probability data obtained in the direct-reaction fission-correlation measurement, ^{234}U(t,pf), to an estimated neutron-induced fission cross section $\sigma[^{235}\mathrm{U}(n,f)]$. The deduced cross section is reproduced in Fig. 1, and compared to the accepted values in the evaluated nuclear data file (ENDF/B-VI) [2]. The ENDF/B-VI evaluation in this case is based on the covariance analysis of experimental data, and is thought to be accurate within 2% in the neutron energy range displayed. This model contains corrections to the fission probabilities due to the difference in the angular-momentum distributions excited in the (t,pf) and (n,f) reactions. Estimated (n,f) cross sections were then obtained by multiplying the fission probabilities with calculated neutron-compound-nucleus formation cross sections for each spin/parity in the compound system, and summing these partial contributions. In both the previous paper and the present work, the ENDF/B-VI compilation has been used as a benchmark because it incorporates recent measurements of (n,f) cross section, where they are available, or reasonable calculations where there are no experimental data. For neutron energies above about 0.5 MeV, the ^{235}U(n,f) results showed agreement to within the estimated $\pm 10\%$ uncertainty quoted for the (t,pf) fission-probability results [3–5]. For energies in the 0.1–0.5 MeV range, the estimated cross sections tended to exceed established ENDF/B-VI values by up to 20%. It was not clear whether the discrepancy at the lower incident neutron energies was due to limitations in the neutron-compound-nucleus formation cross sections or to the correction factors for the different angular-momentum distributions in (t,pf) and (n,f) reactions.

There is a large amount of fission-probability data available for a wide range of actinide nuclei. In earlier (t,pf) experiments [3–5], data were obtained on a series of Th, U, and Pu isotopes, and a simplistic model was used to convert these fission probabilities to estimated (n,f) cross sections for neutron energies in the range 1–2 MeV [6]. The ^{235}U test discussed above showed that the current model [1] could improve on these cross-section estimates and extend the applicable neutron energy range to 0.1–2.2 MeV. The surrogate targets available in the (t,pf) datasets [3–5] are shown in Table I. There are five cases (^{234,235,236}U and ^{240,241}Pu) where high-quality direct measurements of the (n,f) cross section can be used to further test the technique. For ^{237}U ($T_{1/2} = 6.8$ days), several very difficult experiments [7,8,10,11] have yielded inconsistent data with large uncertainties and so there is a significant question as to the magnitude and shape of this cross section. The remaining cases (^{231,233}Th, ^{239}U, and ^{243}Pu) with half lives from minutes to hours cannot be measured directly, but their fission cross sections could be important in environments where multiple neutron captures are possible on a short time scale.

In this paper, we obtain estimated (n,f) cross sections for targets of ^{240,241,243}Pu, ^{234,236,237,239}U, and ^{231,233}Th in the neutron energy range 0.1–2.2 MeV. Where possible, results are compared to the ENDF/B-VI [2] evaluation to estimate the reliability of the method. The ^{237}U case is discussed in detail and the overall systematics of (n,f) cross sections in this region are presented. Tabulated values of the fission-probability data and deduced (n,f) cross sections are being made available separately [12].

II. EXPERIMENTAL DETAILS

The data used in this paper were taken from work by Britt *et al.* [3] in the case of the ^{234}U(t,pf) reaction, from Cramer and Britt [4] for the ^{230,232}Th(t,pf), ^{236,238}U(t,pf), and ^{240,242}Pu(t,pf) reactions, and from Britt and Cramer [5] for the ^{233,235}U(t,pf) and ^{239}Pu(t,pf) studies. In some cases,

*Electronic address: younes@llnl.gov

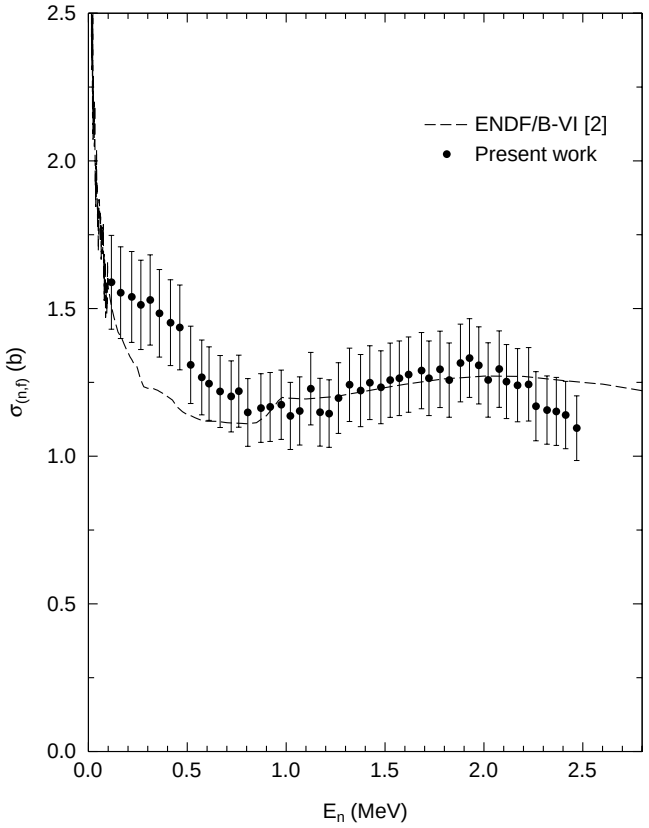

FIG. 1. Plot of the ^{235}U(n,f) cross section deduced from ^{234}U(t,pf) data in Ref. [1] and compared to the ENDF/B-VI evaluation.

the excitation-energy scale of these datasets has been shifted, generally within experimental uncertainties, to match the fission-probability data measured by Back *et al.* [13,14]. The Back *et al.* data were calibrated more precisely, but are not optimized for the surrogate-reaction technique applied in this work. In the most extreme case, the ^{239}Pu(t,pf) data were shifted up in energy by 200 keV, a significant amount compared to the ± 50 keV uncertainty quoted for the original data. For more details on the energy shifts, see Back *et al.* [13].

In all cases the fission probability was measured as a function of excitation energy in the compound system formed by the direct (t,p) reaction. ''Singles'' events corresponding to the detection of the outgoing proton were recorded along with coincidences between detected proton and fission-fragment signals. The ratio of the number of coincidence to singles events, corrected for detection efficiency, gives the probability that the compound system formed by the (t,p) reaction will subsequently fission. The excitation energy of the fissioning nucleus is reconstructed from the measured proton energy and the kinematics of the reaction.

In practice, the singles data were contaminated over localized energy ranges by protons resulting from (t,p) reactions on the carbon backing used to support the actinide samples, and from oxygen nuclei present in the actinide-oxide target layer. A background subtraction was applied to the singles data to eliminate the effect of the contaminants, but contributed to a systematic $\pm 10\%$ uncertainty on all the fission-probability values used in this work.

TABLE I. List of neutron targets and their properties studied by the surrogate (t,p) reaction in this work.

Neutron target	J^π	$T_{1/2}$
^{231}Th	$5/2^+$	25.52 h
^{233}Th	$1/2^+$	22.3 min
^{234}U	0^+	2.455×10^5 yr
^{235}U	$7/2^-$	7.038×10^8 yr
^{236}U	0^+	2.342×10^7 yr
^{237}U	$1/2^+$	6.75 days
^{239}U	$5/2^+$	23.45 min
^{240}Pu	0^+	6564 yr
^{241}Pu	$5/2^+$	14.290 yr
^{243}Pu	$7/2^+$	4.956 h

III. MODEL OVERVIEW

The model used in this paper to deduce the (n,f) cross section from surrogate (t,pf) fission-probability data is described in detail in Ref. [1]. For convenience, the important aspects of the technique are summarized here.

The (t,pf) reaction is assumed to proceed in two sequential steps: first a compound system is formed by a direct (t,p) reaction and then, after a comparatively long time, the equilibrated nucleus fissions. In an earlier work by Cramer and Britt [6], the neutron-induced fission cross section was deduced from measured (t,pf) fission probabilities $P_{(t,pf)}$ as a function of excitation energy E_x of the compound system by simple multiplication with a calculated neutron-compound cross section $\sigma_{CN}(E_n)$:

$$\sigma_{(n,f)}(E_n)=\sigma_{CN}(E_n)P_{(t,pf)}(E_x), \tag{1}$$

where the incident neutron energy E_n is related to the excitation energy E_x of the compound system by $E_n=E_x-B_n$, with B_n the neutron binding energy. The compound cross section $\sigma_{CN}(E_n)$ was calculated using the code ABACUS and accepted optical-model parameters [6]. At that time, it was thought that the compound cross section implied by the ABACUS calculation was overestimated below $E_n \approx 1$ MeV, and in later efforts to extract (n,f) cross sections from ^{3}He-induced surrogate reactions [15], a constant 3.1 b value was used at all energies for $\sigma_{CN}(E_n)$ instead (see Fig. 2). In addition, Eq. (1) makes no provision for the different spin and parity distributions transferred by (t,p) and neutron-induced reactions, respectively.

In the present, improved approach, the (t,pf) fission probabilities are calculated as a function of excitation energy E_x by summing the contributions from individual J^π compound states. The individual J^π components are obtained from the direct-reaction (t,p) population probabilities $P_{(t,p)}$ and the probability P_f of fission from a given state (E_x,J^π) using

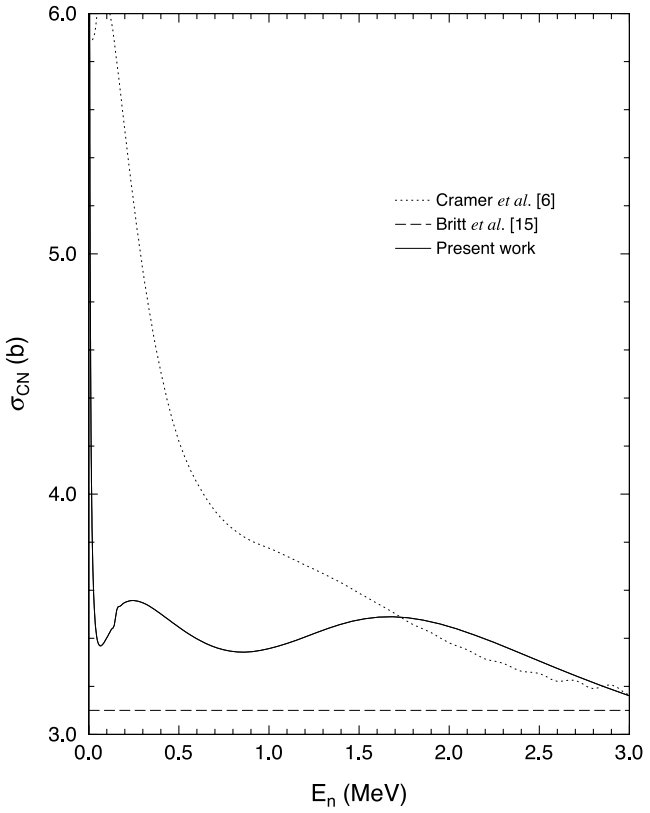

FIG. 2. Compound-nucleus cross section for the neutron-capture reaction calculated in the present work using transmission coefficients from Dietrich [17] and from older ABACUS results, compared to the constant 3.1-b cross section used by Britt *et al.* Note the offset zero in the ordinate scale.

$$P_{(t,pf)}(E_x)=\sum_{J^\pi} P_{(t,p)}(J^\pi)P_f(E_x,J^\pi). \tag{2}$$

The (t,p) population probabilities $P_{(t,p)}(J^\pi)$ are calculated in a distorted-wave Born approximation approach, and they are essentially independent of excitation energy over the energy range of interest. The fission-probability components $P_f(E_x,J^\pi)$ are obtained using the double-humped-barrier statistical fission model summarized in Fig. 3, reproduced from Ref. [1]. The $P_f(E_x,J^\pi)$ values are calculated assuming statistical competition between three possible decay paths from a given compound state: γ decay, neutron emission, and fission. A correction for neutron- and fission-width fluctuations [16] is included but does not have a significant effect on the final estimate of the (n,f) cross section. The γ-decay channel is assumed to proceed via statistical electric dipole transitions. (Partial widths for magnetic dipole radiation are typically weaker than the corresponding electric dipole widths by several orders of magnitude, and have been neglected in the present calculations.) The neutron-emission channel is calculated using transmission coefficients obtained by making a coupled-channel calculation [17]. The neutron-compound cross section calculated using these transmission coefficients is in better agreement with the constant 3.1-b cross section successfully used in Ref. [15] than the earlier ABACUS result (Fig. 2). The fission channel is

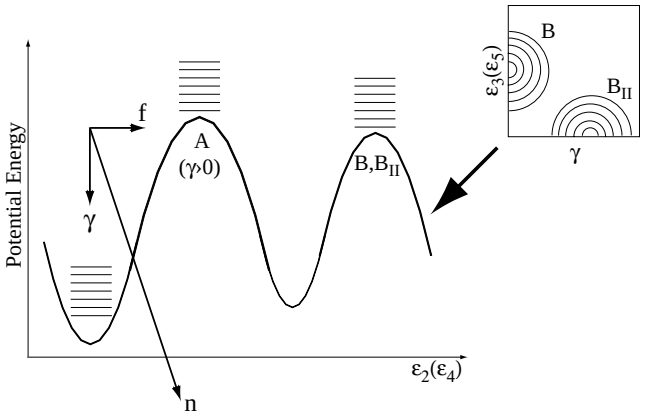

FIG. 3. Schematic representation of the statistical fission model used. The inset shows the difference between barriers B and B_{II} encountered along parallel fission paths: barrier B has a static octupole deformation, whereas barrier B_{II} is triaxial.

treated in a standard Hill-Wheeler formalism that implements the schematic representation in Fig. 3. In this picture, the fissioning nucleus traverses an inner barrier A with triaxial symmetry, and proceeds through one of the two parallel fission paths, through a reflection-asymmetric barrier B or another triaxial barrier B_{II}. Fission through the combined barriers is given by a nonresonant penetration formula.

For each of the decay channels, and for the three barriers in the fission channel, the calculation incorporates a set of experimental discrete levels up to the pairing gap and a continuous level density above the pairing gap. The level density is obtained from the permutation of particles in the shell-corrected single-particle spectra at the appropriate saddle and ground state configurations, using a Strutinsky renormalization process. In the present calculations, the same set of discrete states was used on top of the fission barriers for each actinide. These discrete transition states were deduced from experimental measurements, and have been augmented by generating two-phonon states through the harmonic coupling of the one-phonon levels. The transition states are given explicitly in Fig. 3 of Ref. [1]. Discrete states in the first wells were taken from the evaluated nuclear structure data file (ENSDF) [18], compiled from experimental results. Where the ENSDF data are insufficient, rotational bands have been extended up to the pairing gap using a standard axial-rotor formulation of the band-member energies.

Once the fission-probability components $P_f(E_x,J^\pi)$ are calculated, the (n,f) cross section is obtained by folding them with a neutron-compound cross section σ_{CN} calculated with the same transmission coefficients used in the description of the neutron-emission channel,

$$\sigma_{(n,f)}(E_n)=\sum_{J^\pi} \sigma_{CN}(E_n,J^\pi)P_f(E_x,J^\pi). \tag{3}$$

The model described above was constructed to incorporate the important physical aspects of the formation and fission processes, with a minimum of adjustable parameters. In fact, only the heights of barriers A and B have been opti-

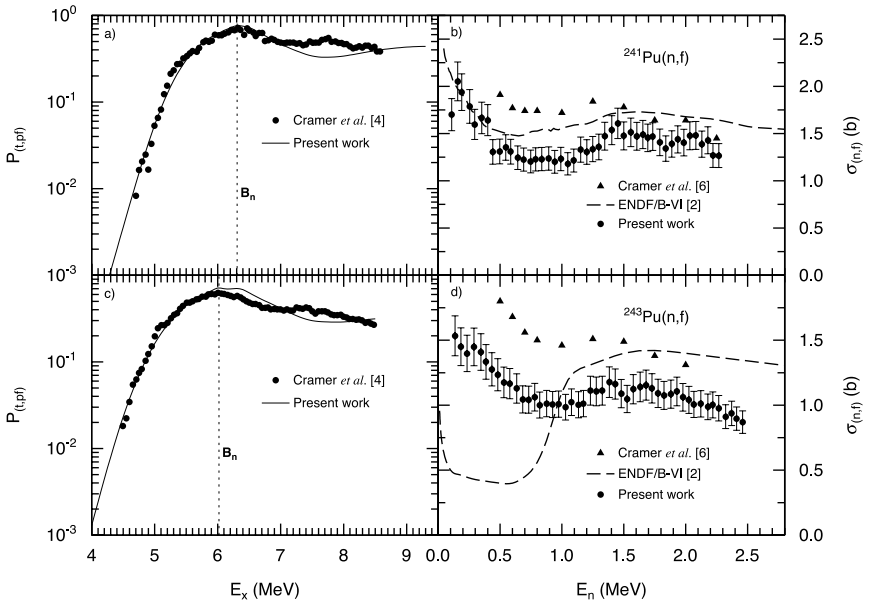

FIG. 4. Best fits (solid curves) to $P_{(t,pf)}$ data (filled circles) for (a) ^{240}Pu(t,pf) and (c) ^{242}Pu(t,pf) measurements, and the correspondingly deduced (b) ^{241}Pu(n,f) and (d) ^{243}Pu(n,f) cross sections, respectively. In panels (a) and (c), the vertical dotted line marks the position of the neutron binding energy for the compound system. Comparisons to estimated (n,f) cross sections by Cramer and Britt and to the ENDF/B-VI evaluation are also shown in panels (b) and (d).

mized in the present work to reproduce the measured fission probabilities up to the neutron binding energy. A price must be paid for such a constrained approach and, indeed, the mismatch between discrete levels and continuous level-density formulations becomes apparent as oscillations in the fits to many of the $P_{(t,pf)}$ datasets above $E_x = B_n$. In order to compensate for this limitation, a renormalization procedure has been devised, which is thoroughly described in Ref. [1]. Thus, the (n,f) cross sections in Eq. (3) are multiplied by the ratio of measured to calculated $P_{(t,pf)}$ values. It was shown in Ref. [1] in the case of the ^{235}U(n,f) cross section deduced from ^{234}U(t,pf) data that the results are made more reliable and more robust by this renormalization procedure. In effect, the renormalization process produces a correction factor to Eq. (1) that depends on the differences in angular-momentum distributions in the (t,pf) and (n,f) reactions. All the (n,f) cross sections presented in this paper have been renormalized in this manner.

For all but the thorium case, the height of the parallel outer barrier B_{II} was not adjusted in the present calculation but, rather, was fixed at 6.40 MeV, the value established for ^{238}U in Ref. [19]. For the Th calculations, the model was slightly modified to accommodate the known anomaly in the barrier shape. Both barriers *A* and *B* were taken to be reflection-asymmetric in shape, with the appropriate modifications to the discrete levels and continuous level densities built on top of the barriers, and barrier B_{II} was eliminated altogether.

In the case of the even-*A* neutron targets, ^{240}Pu, ^{234}U, and ^{236}U, no discrete levels were used in the model, and the calculated continuous level-density functions were extended below the pairing gap instead. In addition, barrier heights were not adjusted to fit the $P_{(t,pf)}$ data in those cases, but instead were taken directly from an earlier work [20].

IV. RESULTS

The aim of the present work is to deduce the (n,f) cross sections from (t,pf) data, but not necessarily to produce a more current set of barrier heights for the actinide nuclei discussed here. To this end, a simplified, nonresonant version of the double-humped fission-barrier model has been used that averages out any resonant structures observed below the neutron binding energy. Therefore, the barrier heights obtained here cannot be taken literally. The renormalization technique introduced in Ref. [1], and repeated in Sec. III, compensates for limitations of the simplified model used here.

In this section, results for simulated (n,f) cross sections on targets of ^{240,241,243}Pu, ^{234,236,237,239}U, and ^{231,233}Th will be presented, discussed, and compared to ENDF/B-VI [2], where possible. In a following section, the systematics and reliability of the estimated cross sections will be investigated.

A. ^{241}Pu(n,f)

Results for the simulated ^{241}Pu(n,f) reaction are shown in Fig. 4. In this case, an extensive set of direct measurements exists. A comparison to the evaluated dataset ENDF/B-VI is shown. The estimated cross section is approximately 15% below the ENDF/B-VI in the neutron energy region above 0.5 MeV.

The appearance of some gross structure in the region near $E_n = 1.5$ MeV is within the estimated systematic errors and may well be due to uncertainties in the determination of Pu singles distributions in the vicinity of C and O contaminants.

The previous estimates of Cramer and Britt [6] are also shown in Fig. 4, and the present results are systematically lower. This is primarily due to the improved calculations for the neutron-compound-nucleus formation cross section. Similar deviations from the Cramer and Britt estimates will be seen in the other cases presented below.

B. ^{243}Pu(n,f)

Results for the simulated ^{243}Pu(n,f) reaction are shown in Fig. 4. In this case the ENDF/B-VI file is also plotted, but

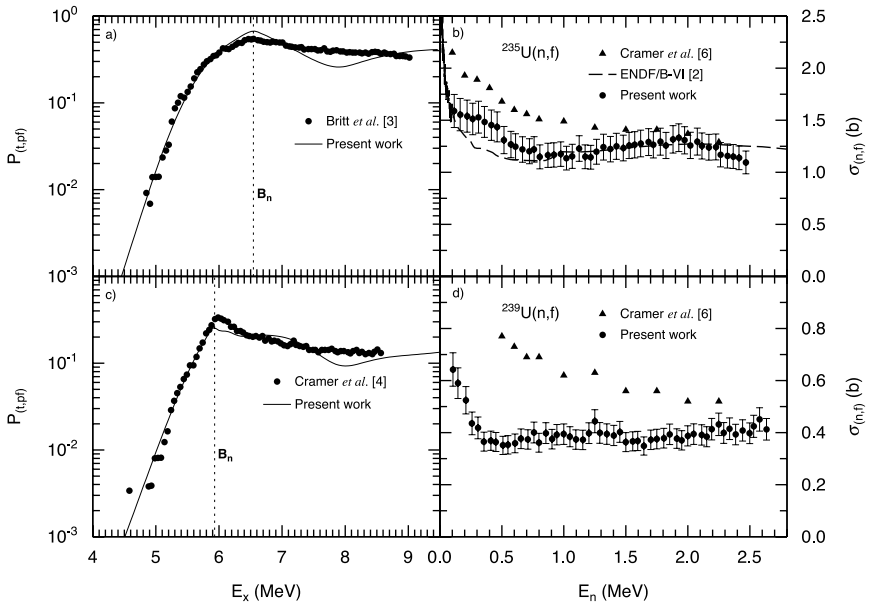

FIG. 5. Same as in Fig. 4, but for (a) $^{234}\mathrm{U}(t,pf)$ and (c) $^{238}\mathrm{U}(t,pf)$ measurements, and the correspondingly deduced (b) $^{235}\mathrm{U}(n,f)$ and (d) $^{239}\mathrm{U}(n,f)$ cross sections, respectively.

there have been no direct ^{243}Pu measurements of the cross section due to its short half-life of 5 h. The ENDF/B-VI file is obviously a calculation that bears little relationship to the real cross section, except maybe for $E_n > 1$ MeV. The estimate of Cramer *et al.* for the (n,f) cross section lies higher than the present result, again due to the limitations of the optical-model calculation.

C. $^{235}\mathrm{U}(n,f)$

Results for the simulated $^{235}\mathrm{U}(n,f)$ cross section are shown in Fig. 5. These are the same results as in Fig. 9 of Ref. [1], and are included here for completeness. The estimated cross section is in very good agreement with ENDF/B-VI. Above $E_n = 0.5$ MeV, the agreement is essentially within the $\pm 10\%$ systematic uncertainty of the data of Britt *et al.* [3]. Below 0.5 MeV, the present result exceeds the ENDF/B-VI evaluation, which is thought to be accurate to within 2% below $E_n = 3$ MeV, by 20% at most. Note that this remarkable agreement between deduced and accepted cross sections is achieved even though the $P_{(t,pf)}$ data are not perfectly reproduced by the fission model calculation in Fig. 5(a). The success of the surrogate technique in spite of this limitation can be attributed to the renormalization scheme discussed in Sec. III.

D. $^{237}\mathrm{U}(n,f)$

Results for the $^{237}\mathrm{U}(n,f)$ cross section are shown in Fig. 6. There has been considerable interest in ^{237}U, but previous measurements were extremely difficult to analyze due to its short half-life of 6.8 days. Figure 6 includes data reported by McNally *et al.* [7] and Cowan *et al.* [10]. The data of McNally *et al.* were obtained using an underground nuclear explosion as an intense neutron source, and the measurements of Cowan *et al.* relied on neutron sources with a spectrum peaked near 200 keV. In addition there was a critical-assembly measurement by Barr [8], which appeared to conflict with the McNally results. The ENDF/B-VI file follows the McNally data at low neutron energies and the Cramer [4] results at energies above 1 MeV. The ENDF/B-VII evaluation [9], which was generated without prior knowledge of our work, is consistent with the Cramer values for $E_n > 1$ MeV, and agrees with the present results near $E_n = 0.5$ MeV. The estimated cross section from the present work is a reevaluation of the Cramer result. It is somewhat lower and flatter with a mean value of about 0.5 b for neutron energies above 0.5 MeV, as compared to the previous accepted value [2] of about 0.7 b.

The comparison of the three previous experiments with the present result and with theoretical calculations by Lynn and Hayes [21] has been discussed in detail in a separate report [11]. A summary is included here. Below 0.5 MeV, the McNally [7], Cowan [10], and present results are in reasonable agreement. The average cross section in the present work, taken over the range $E_n = 0.1$–0.4 MeV, is 0.8 times the McNally values, well within the uncertainties of the McNally experiment. Above $E_n = 0.5$ MeV, the McNally values rise sharply. The critical assembly experiment [8] measured a ratio of integral ^{237}U and ^{235}U neutron cross sections, averaged over a range of neutron energies, with ^{237}U material from the same batch as was used in the direct McNally measurement. The critical-assembly neutron spectrum was peaked at about 100 keV with significant flux extending out to about 2 MeV. The experimental value obtained for the integral $^{237}\mathrm{U}/^{235}\mathrm{U}$ cross-section ratio was 0.391 ± 0.012. However, when the same ratio was calculated with the critical-assembly spectrum, and assuming the McNally fission cross section, a value of 0.62 was obtained, in disagreement with the measured 0.391 result. Using the present results for the $^{237}\mathrm{U}(n,f)$ cross sections and the same neutron spectrum as McNally in Ref. [7] yields a ratio of 0.43, which is 10% higher but in reasonable agreement with the measured [8] critical-assembly value of 0.391. It has been assumed that the discrepancy between the critical assembly and McNally integral ratio was due to problems with the McNally results at high incident neutron energies, as re-

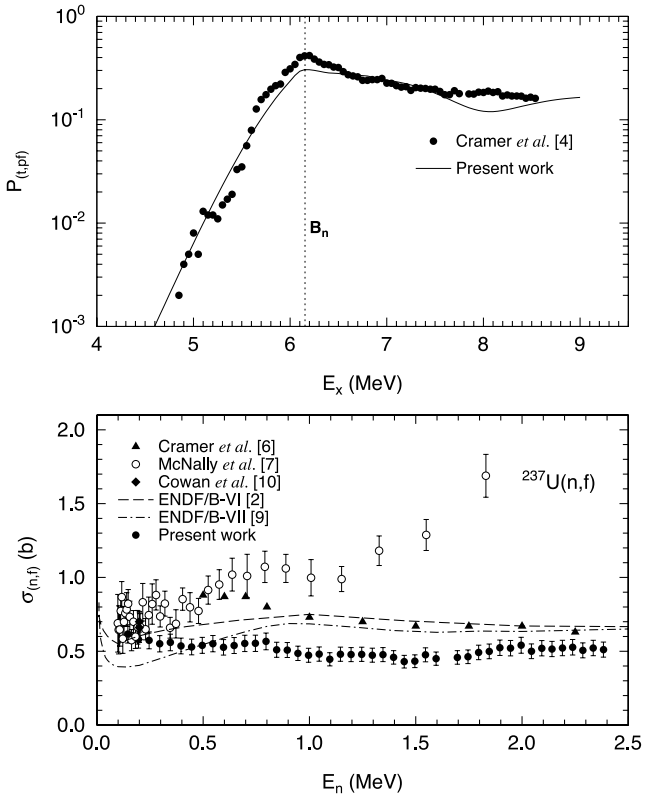

FIG. 6. The top panel shows the best fit (solid curve) to measured $^{236}\mathrm{U}(t,pf)$ fission-probability data (filled circles). The vertical dotted line marks the position of the neutron binding energy for the compound system. The bottom panel shows the deduced cross section compared to data from McNally *et al.* and Cowan *et al.*, and to the deduced cross section from an earlier analysis of the same $P_{(t,pf)}$ data by Cramer and Britt. The ENDF/B-VI and ENDF/B-VII evaluations are also plotted for comparison.

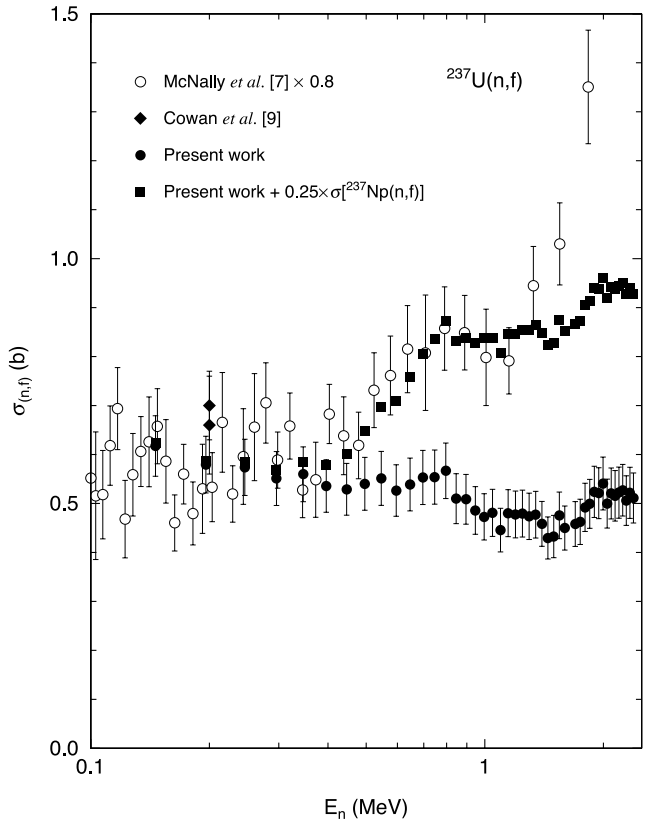

FIG. 7. Effect of scaling the $^{237}\mathrm{U}(n,f)$ cross section of McNally *et al.* by a multiplicative factor of 0.8 to match the present results below $E_n=0.4$ MeV, and adding a 25% contribution from the contaminant $^{237}\mathrm{Np}(n,f)$ cross section.

flected in the ENDF/B-VI evaluation. Based on the present new results and previous measurements below $E_n=0.5$ MeV, the likely explanation for this discrepancy is the presence of a larger contribution from ^{237}Np (the β-decay daughter of ^{237}U) than the McNally group originally estimated. In the surrogate $^{236}\mathrm{U}(t,pf)$ measurement, a 99.88%-enriched sample of ^{236}U was used, with a negligible 0.12% ^{235}U contamination [4]. Figure 7 shows a plot of the $^{237}\mathrm{U}(n,f)$ cross section deduced in this paper with an addition of 25% of the $^{237}\mathrm{Np}(n,f)$ cross section (taken from Ref. [2]) compared to the McNally results renormalized by a factor of 0.8 to match the present results below 0.4 MeV. The McNally *et al.* values are reasonably well reproduced by this procedure. In a theoretical prediction of the $^{237}\mathrm{U}(n,f)$ cross section, Lynn and Hayes [21] chose to address this problem by renormalizing the McNally results to match the critical-assembly integral value. However, based on the arguments above, we believe that the estimated cross sections from the (t,pf) surrogate reaction obtained from the present work are the most reliable for the $^{237}\mathrm{U}(n,f)$ reaction.

E. $^{239}\mathrm{U}(n,f)$

Results for the $^{239}\mathrm{U}(n,f)$ simulation are shown in Fig. 5. For this case, direct measurements are practically impossible due to the short half-life (23 min), and there is no ENDF/B-VI file for the $^{239}\mathrm{U}(n,f)$ reaction. The $^{238}\mathrm{U}(t,pf)$ surrogate reaction is the only experimental technique available to estimate the $^{239}\mathrm{U}(n,f)$ cross section, and the results presented here should be reliable and accurate within the global systematic uncertainties discussed in Sec. V.

F. $^{231}\mathrm{Th}(n,f)$

The thorium nuclei represent a special class of systems where the barrier structure is not well understood. The treatment of the fission barriers in the $^{231,233}\mathrm{Th}(n,f)$ calculations is discussed in Sec. III.

Results for ^{231}Th are shown in Fig. 8. Direct measurements are practically impossible due to the short half-life (25.5 h), and again there is no corresponding ENDF/B-VI file. The results presented here should be reliable and accurate within the global systematic uncertainties discussed in Sec. V.

G. $^{233}\mathrm{Th}(n,f)$

Results for the $^{233}\mathrm{Th}(n,f)$ reaction are shown in Fig. 8. For this case, the barrier-height values that fit the data below $E_x=B_n$ do not reproduce the data above B_n. The reason for this discrepancy is not clear but it may be due to an improper modeling of the barrier structure, as discussed in Sec. III.

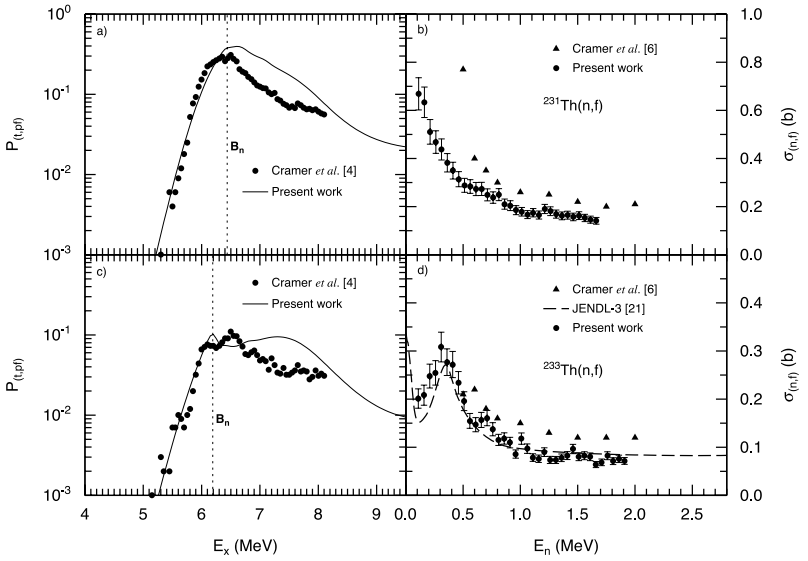

FIG. 8. Same as in Fig. 4, but for (a) ^{230}Th(t,pf) and (c) ^{232}Th(t,pf) measurements, and the correspondingly deduced (b) ^{231}Th(n,f), and (d) ^{233}Th(n,f) cross sections, respectively.

However, the renormalization procedure should still yield reliable estimates for the (n,f) cross section.

In this case as well, direct measurements of the ^{233}Th(n,f) cross section are practically impossible due to the short half-life (22.3 min). There is no corresponding ENDF/B-VI file. There is, however, a file in the JENDL-3 database [22] which agrees very well with the present estimate for the ^{233}Th(n,f) cross section. The source of the JENDL-3 evaluation is not clear, but appears to be based on an analysis of the Cramer ^{232}Th(t,pf) data [4]. The results presented here should be reliable and accurate within the global systematic uncertainties discussed in Sec. V.

H. ^{240}Pu(n,f), ^{234}U(n,f), and ^{236}U(n,f)

There are three even-even nuclei available as neutron targets that can be measured using the surrogate technique on corresponding even-odd targets. For ^{240}Pu, ^{234}U, and ^{236}U, target material for direct (n,f) measurements is readily available. Thus, these cases provide another validation of the technique in a different class of nuclei. Figure 9 shows results for the simulated (n,f) reactions. In these calculations, the previously determined barrier parameters [20] were used with no adjustment. As shown in detail in the previous ^{235}U paper, the renormalization to the experimental (t,pf) fission probabilities corrects for any inadequacies in the fit to the measured $P_{(t,pf)}$ values.

Figure 9 shows that the simulated (n,f) cross sections compare quite well with the ENDF/B-VI files, which are based on extensive direct (n,f) experiments. ^{240}Pu and ^{234}U tend to drop slightly below the ENDF/B-VI values at the higher end of the energy range, while in ^{236}U there is a similar deviation in the middle of the energy range. The direct (n,f) measurements evaluated in ENDF/B-VI are taken as a reliable reference, and the deviation of the surrogate results from these reference values will be used in Sec. V to quantify the systematic uncertainties in the (n,f) cross sections obtained here.

V. DISCUSSION

In this section, the comparisons to the ENDF/B-VI evaluation wherever possible will be discussed. The relation of these results to the earlier attempt by Cramer-Britt [6] to estimate (n,f) cross section from surrogate (t,pf) reactions using the same datasets utilized in this work, but with a simpler procedure described in Sec. III, will also be presented.

A. ENDF/B-VI

For the purposes of this paper, the ENDF/B-VI evaluation is taken as the ''gold standard'' of currently accepted cross sections. It should be noted that, the ENDF/B-VI cross sections used here are often quoted in the database without uncertainties, with the exception of the ^{235}U(n,f) cross section, which is thought to be known to better than 2% for $E_n < 3$ MeV.

Table II presents comparisons of averaged surrogate and ENDF/B-VI data for the five cases where the ENDF/B-VI evaluations exist. For a global comparison, an average was taken in the region $1 < E_n$ (MeV) < 3, where the (n,f) cross sections are all relatively constant with respect to incident neutron energy. For targets of ^{234}U, ^{235}U, and ^{240}Pu, the deduced (n,f) cross sections differ from the accepted ENDF/B-VI results by less than the estimated $\pm 10\%$ systematic uncertainty quoted in Refs. [4,5]. Deviations in two cases, ^{236}U and ^{241}Pu, are slightly larger and of opposite sign $(+13.5\%$ and $-14.6\%)$, respectively. These values and their scatter fit well with the estimated $\pm 10\%$ uncertainty estimate, if that estimate is taken as a standard deviation. It should be noted that this discussion does not address uncertainties in the evaluated ENDF/B-VI cross sections, which are difficult to discern [except in the case of the ^{235}U(n,f) cross section]. In addition to the global comparison, localized differences in shape between the ENDF/B-VI and surrogate cross sections can be seen in Figs. 4–6 and 9. The differences in shape in the region below $E_n = 0.5$ MeV or so are in the $\pm 20\%$ range. Above $E_n = 0.5$ MeV, the observed

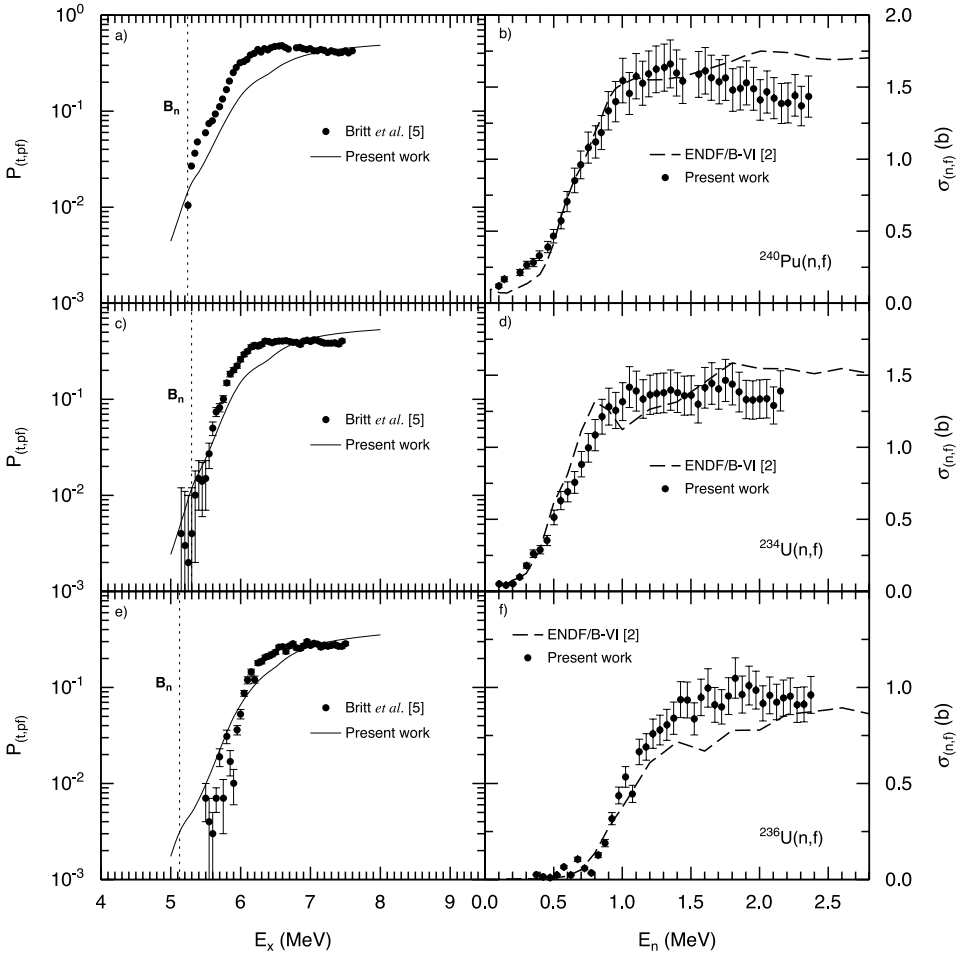

FIG. 9. Calculated (solid curves) and measured $P_{(t,pf)}$ values (filled circles) for the (a) ^{239}Pu(t,pf), (c) ^{233}U(t,pf), and (e) ^{235}U(t,pf) reactions, and the correspondingly deduced (b) ^{240}Pu(n,f), (d) ^{234}U(n,f), and (f) ^{236}U(n,f) cross sections, respectively. The $P_{(t,pf)}$ calculations in panels (a), (c), and (e) were performed using previously established barrier-height values [15]. In panels (a), (c), and (e) the vertical dotted line marks the position of the neutron binding energy for the compound system. Comparisons to the ENDF/B-VI evaluation are shown in panels (b), (d), and (f).

discrepancies could be due to the additional uncertainties in the (t,pf) singles data in narrow energy regions where reactions on C and O contaminants contribute peaks that obscure the measured actinide (t,p) cross section. Below $E_n = 0.5$ MeV for the two thermal fissioning targets, ^{235}U and ^{241}Pu, there is a tendency for the surrogate results to rise more rapidly than the ENDF/B-VI data with decreasing neutron energy. This effect is much less pronounced than in previous attempts to deduce the (n,f) cross section where inadequate neutron-compound-nucleus formation cross sections were used [6]. These residual discrepancies could be due either to uncertainties in the compound cross sections, or to limitations in the correction for the angular-momentum mismatch between (n,f) and (t,pf) reactions.

TABLE II. Average cross sections for $1 \leqslant E_n$ (MeV) $\leqslant 3$ obtained in the present surrogate work ($\overline{\sigma}^{(\mathrm{surr})}_{(n,f)}$) compared to the ENDF/B-VI evaluation ($\overline{\sigma}^{(\mathrm{endf})}_{(n,f)}$).

Neutron target	$\overline{\sigma}^{(\mathrm{surr})}_{(n,f)}$ (b)	$\overline{\sigma}^{(\mathrm{endf})}_{(n,f)}$ (b)	Relative deviation (%)
^{234}U	1.37	1.45	−5.5
^{235}U	1.23	1.23	0.0
^{236}U	0.87	0.77	+13.5
^{240}Pu	1.51	1.61	−6.2
^{241}Pu	1.40	1.64	−14.6

B. Comparison to Cramer-Britt (n,f) estimates

In a previous paper [6], Cramer and Britt attempted to estimate the (n,f) cross sections for the even-odd nuclei presented here using the same (t,pf) datasets. As is discussed in more detail in Ref. [1], the correction for the different angular-momentum distributions in (t,p) and neutron-induced reactions, which is most important below $E_n = 0.5$ MeV, allows the current surrogate technique to be used down to the energy resolution limit of the experiment, 0.1 MeV. The present results also differ from the earlier Cramer-Britt estimates because of a much improved set of calculated compound-nucleus formation cross sections [17] for the neutron channels. The success of the surrogate technique, where a comparison with independent measurements is possible, is evidence for the accuracy of the calculated neutron transmission coefficients.

VI. SUMMARY

We have presented a reliable set of estimated (n,f) cross sections for several thermally fissionable actinide nuclei that are ''unmeasurable'' by direct techniques due to lifetime limitations of appropriate target material. Based on the com-

parison with five independently measured (n,f) cross sections, the surrogate technique appears to be reliable within the estimated uncertainties of the (t,pf) data sets (10% globally and 20% locally). Within this accuracy range, the calculated neutron-compound cross sections appear adequate, with the possibility that some improvements might be achieved below $E_n=0.5$ MeV. In addition to the (t,p) data discussed in this paper, fission-probability measurements exist for a variety of other, mostly odd-Z, nuclei, primarily from ^{3}He-induced reactions. In a subsequent paper, the present model will be extended to handle ^{3}He-induced reactions and update the earlier attempt of Britt and Wilhelmy [15] to estimate (n,f) cross sections on targets of ^{230,231}U, $^{232-238}$Np, ^{236,237}Pu, and $^{238-244}$Am. These datasets are interesting because they provide fission-probability data up to much higher energies than has been possible in the (t,pf) experiments (e.g., up to $E_n\approx 6$ MeV). With a more extensive range of neutron energies, certain aspects of the current model, such as the continuous level-density formulations, can be more thoroughly refined and tested.

The main limitations of the present results are the uncertainties in the (t,pf) data and the fact that the datasets only extend to 2.2 MeV. The energy resolution in the experimental data imposes a lower limit for the technique at about $E_n=0.1$ MeV. The upper limit of $E_n\approx 2.2$ MeV was taken to stay below the triton breakup energy but, in practice, was also dictated by the contamination of the singles spectra by C and O peaks. At present there are no triton beams available in the world, and the Cramer experiment cannot be repeated or improved upon. However, in at least a few cases, the experiments could be revisited in inverse kinematics with actinide beams from a fragmentation facility. The singles-contaminant problem endemic to previous (t,pf) experiments could be mitigated in inverse-kinematics measurements. Depending on the construction of the tritium targets and the detector geometry, the contaminant peaks can be shifted to more propitious energies. The inverse techniques have yet to be developed but they will clearly be important in future attempts to deduce neutron cross sections on unstable elements produced at a radioactive beam facility.

Another possibility for a two-neutron transfer reaction would be $(^{18}O,^{16}O)$. However, this is likely to be more difficult than using the (t,p) reaction. Since most of the cross sections tend to be contained in a momentum-matching "Q-value window" [23], which is likely to be narrower for $(^{18}O,^{16}O)$ than for the (t,p) reaction, the usefulness of the heavy-ion transfer reaction will depend on where this window falls relative to the fission-barrier heights. Furthermore, a better energy resolution can be achieved with the (t,p) reaction, compared to the $(^{18}O,^{16}O)$ reaction. To our knowledge, the surrogate $(^{18}O,^{16}Of)$ reaction has not been attempted and, in spite of potential experimental difficulties, is worth considering as an alternative to the (t,pf) reaction.

ACKNOWLEDGMENTS

Valuable input on this project came from continuing discussions with John A. Becker, Jerry B. Wilhelmy, Frank S. Dietrich, and Dennis P. McNabb. This work was performed under the auspices of the U.S. Department of Energy by the University of California, Lawrence Livermore National Laboratory under Contract No. W-7405-Eng-48.

[1] W. Younes and H.C. Britt, Phys. Rev. C **67**, 024610 (2003).
[2] Cross Section Evaluation Working Group, National Nuclear Data Center, Report BNL-NCS-17541 (ENDF-201), 1991 (unpublished).
[3] H.C. Britt, F.A. Rickey, and W.S. Hall, Phys. Rev. **175**, 1525 (1968).
[4] J.D. Cramer and H.C. Britt, Phys. Rev. C **2**, 2350 (1970).
[5] H.C. Britt and J.D. Cramer, Phys. Rev. C **2**, 1758 (1970).
[6] J.D. Cramer and H.C. Britt, Nucl. Sci. Eng. **41**, 177 (1970).
[7] J.H. McNally, J.W. Barnes, B.J. Dropesky, P.A. Seeger, and K. Wolfsberg, Phys. Rev. C **9**, 717 (1974).
[8] D. W. Barr (private communication).
[9] P. G. Young (private communication); P. G. Young and M. B. Chadwick, Report T-16: NW-2/10-00, 2000 (unpublished).
[10] G. A. Cowan, G. A. Jarvis, G. W. Knobeloch, and B. Warren, LASL Report LA-1669, 1955 (unpublished).
[11] W. Younes, H. C. Britt, and J. B. Wilhelmy, LASL Report UCRL-ID-152621, 2003 (unpublished).
[12] W. Younes and H. C. Britt, LLNL Report UCRL-ID-152906, 2003 (unpublished).
[13] B.B. Back, Ole Hansen, H.C. Britt, and J.D. Garrett, Phys. Rev. C **9**, 1924 (1974).
[14] B.B. Back, H.C. Britt, Ole Hansen, B. Leroux, and J.D. Garrett, Phys. Rev. C **10**, 1948 (1974).
[15] H.C. Britt and J.B. Wilhelmy, Nucl. Sci. Eng. **72**, 222 (1979).
[16] B.B. Back, J.P. Bondorf, G.A. Ostroschenko, J. Pedersen, and B. Rasmussen, Nucl. Phys. **A165**, 449 (1971).
[17] F. S. Dietrich (private communication); see more extensive discussion in Ref. [1].
[18] Data extracted using the NNDC On-Line Data Service from the ENSDF database, file revised as of 2/24/03; M. R. Bhat, *Evaluated Nuclear Structure Data File (ENSDF)*, in *Nuclear Data for Science and Technology*, edited by S. M. Qaim (Springer-Verlag, Berlin, Germany, 1992), p. 817.
[19] A. Gavron, H.C. Britt, P.D. Goldstone, J.B. Wilhelmy, and S.E. Larsson, Phys. Rev. Lett. **38**, 1457 (1977).
[20] H. C. Britt, in *Proceedings of the Fourth International Symposium on the Physics and Chemistry of Fission, Julich, West Germany* (International Atomic Energy Agency, Vienna, 1979), Vol. 1, p. 3.
[21] J.E. Lynn and A.C. Hayes, Phys. Rev. C **67**, 014607 (2003).
[22] T. Nakagawa *et al.*, J. Nucl. Sci. Technol. **32**, 1259 (1995).
[23] W. Henning, Y. Eisen, H.-J. Körner, D.G. Kovar, J.P. Schiffer, S. Vigdor, and B. Zeidman, Phys. Rev. C **17**, 2245 (1978).